



Influences of Laser Incidence Angle and Wall Thickness on Additive Components

Alexander J. Wildgoose¹

Department of Mechanical Engineering,
 Pennsylvania State University,
 State College, PA 16801
 e-mail: ajw324@psu.edu

Karen A. Thole

Department of Mechanical Engineering,
 Pennsylvania State University,
 State College, PA 16801
 e-mail: kthole@psu.edu

Additive manufacturing (AM), particularly laser powder bed fusion, is growing the ability to rapidly develop advanced cooling schemes for turbomachinery applications. However, to fully utilize the design and development opportunities offered through AM, impacts of the build considerations and processing parameters are needed. Prior literature has shown that specific build considerations such as laser incidence angle and wall thickness influence the surface roughness of additively made components. The objective of this technical brief is to highlight the effects of both laser incidence angle and wall thickness on the surface roughness and cooling performance in micro-sized cooling passages. Results indicate that for any given laser incidence angle, surface roughness begins to increase when the wall thickness is less than 1 mm for the cooling channels evaluated. As the laser incidence angle becomes further away from 90 deg, the surface roughness increases in a parabolic form. Laser incidence angle and wall thickness significantly impact friction factor, while there is less of an influence on the Nusselt number for additively manufactured microchannels. [DOI: 10.1115/1.4062678]

Keywords: additive manufacturing, heat transfer, laser incidence angle, wall thickness

1 Introduction

The additive manufacturing (AM) process, namely laser powder bed fusion, provides a technology to more rapidly fabricate complex cooling designs, such as those in the hot section of gas turbines, compared to traditional manufacturing techniques. Prior to post-processing, components that are additively manufactured have been shown to exhibit higher levels of surface roughness relative to traditional fabrication (subtractive or casting) methods. Post-processing as-built complex internal AM passages, such as channel shapes with ribs and pin fins, is challenging. Consequently, it is important to understand the influences of manufacturing on roughness and how that affects pressure loss and convective heat transfer.

Examining different geometric shapes made using AM has revealed differences in surface roughness. Wildgoose et al. [1]

observed differences in roughness between the various surfaces of a variety of cross-sectional shapes that were all printed perpendicular to the build plate, which is optimal for minimizing roughness. Of the various channel shapes, the square channel exhibited the highest difference in roughness between the four channel walls compared to other channel shapes, such as the diamond which is essentially a rotated square. The square and diamond channel from the study shared the same hydraulic diameter; however, the surface roughness was higher for two of the surfaces of the square compared to the diamond which had relatively the same roughness on all of its surfaces. A comparison in roughness from a computed tomography (CT) scan of the square channel is shown in Fig. 1(a), and diamond shape is shown in Fig. 1(b). A 3, 6, 9, and 12 o'clock compass is accompanied in Fig. 1, which highlights the orientation and wall thickness for each surface. It would be expected that the roughness of each surface in the cooling channel would be similar between the square and diamond since all surfaces have the same build direction relative to the build plate; however, a key difference between the surfaces of the square and diamond is the wall thickness relative to the external coupon surface.

When examining other work in literature, the results from Wildgoose et al. [2] and Jamshidinia et al. [3] showed wall thickness does impact surface roughness. Wildgoose et al. [2] observed the internal surface roughness levels exponentially increased when the wall thickness values were less than 1.2 mm. The trend of roughness as a function of wall thickness can be seen in Fig. 2, which was adapted from Wildgoose et al. [2]. Surfaces that have a constant wall thickness of 2 mm in Fig. 2 showed minimal change in surface roughness level.

However, wall thickness does not fully describe why the diamond channel contained a lower roughness compared to the square channel, especially since the only difference between the diamond and square is that the diamond is rotated about its axial axis. In addition to wall thickness, when reexamining the cause for various roughness's in the variety of channel shapes from Wildgoose et al. [1], the laser incidence angle (ζ) was different for each cooling sample. The laser incidence angle describes the angle of the laser to that of the sintered surface. Several past studies have reported that changes to laser incidence angle can impact part quality [4–6]. When comparing the channel shapes, the square channel contained the greatest range in laser incidence angles compared to other shapes, such as the diamond in Fig. 1(b). The cause for the diamond to have exhibited a lower roughness relative to the square is that the diamond shape contained a lower laser incidence angle compared to the square. A similar observation with laser incidence angle was observed by Kleszczynski et al. [4], where the further the part was from the laser source, the higher the surface roughness (because of the higher value in laser incidence angle). Several additional studies [5–7] have revealed that the laser incidence angle caused differences in surface quality between parts.

Within the literature, the impact of the wall thickness and laser incidence angle (two parameters) on surface quality and cooling performance have not been discussed together. The goal of this technical brief is to highlight the relationship between laser incidence angle and wall thickness on the roughness and cooling performance of internal passages made through AM.

2 Characterizing Build Parameters and Roughness

The laser incidence angle was calculated for a variety of AM cooling passages that have been previously reported in the literature

¹Corresponding author.

Manuscript received March 9, 2023; final manuscript received May 28, 2023; published online June 26, 2023. Assoc. Editor: Giovanna Barigozzi.

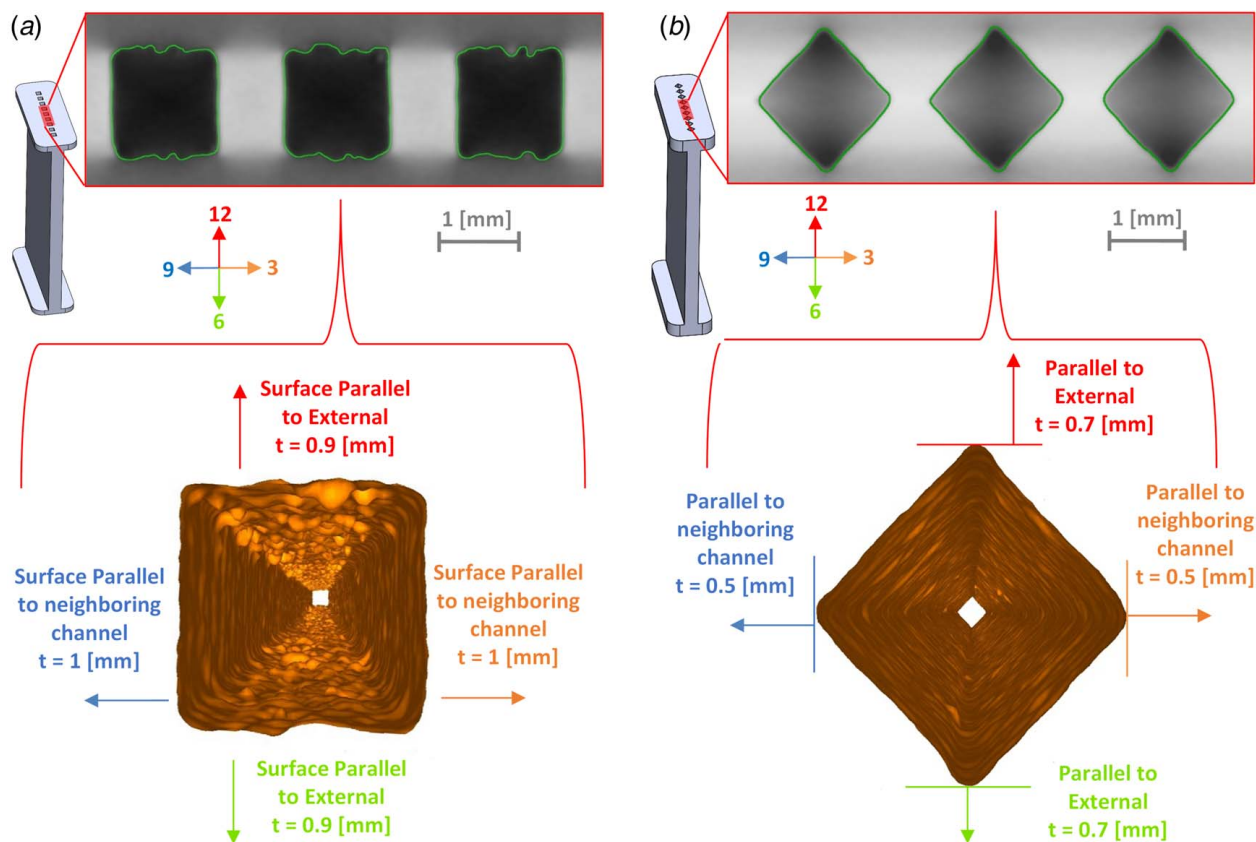


Fig. 1 CT scan of the (a) square channel and the (b) diamond channel highlighting the differences in surface roughness for each surface orientation [1]

[1,2,8]. The cooling passages analyzed contained flat internal surfaces, such as channels with a square cross section. To minimize the effect of build direction on roughness, only cooling channels that were fabricated perpendicular to the build plate (no downward-facing surfaces) were analyzed. The specific geometry and AM build parameters of the Inconel 718 coupons are reported in their respective studies. In general, the design of the cooling coupons evaluated contained multiple noncircular shaped channels, such as the square channel coupon shown in Fig. 1(a).

As shown in Fig. 3, the laser incidence angle is defined as the minimal angle between the laser vector to that of the vector

normal to the part surface (surface vector), which is similar to that of Subramanian et al. [5]. Determining the laser vector is challenging since the laser beam in most AM machines is filtered through multiple lenses and then is focused before it exits the lens cover. An illustration of a general laser setup without the filtering lenses is shown in Fig. 3. Metal AM machines contain different focusing lenses such as a f -theta lens, which causes there to be a different laser vector start point depending upon where the beam entered the f -theta lens from the scanner or prior lens [9]. To simplify the laser vector origin, the starting point of the laser vector was chosen to be the center of the lens cover of the AM machine,

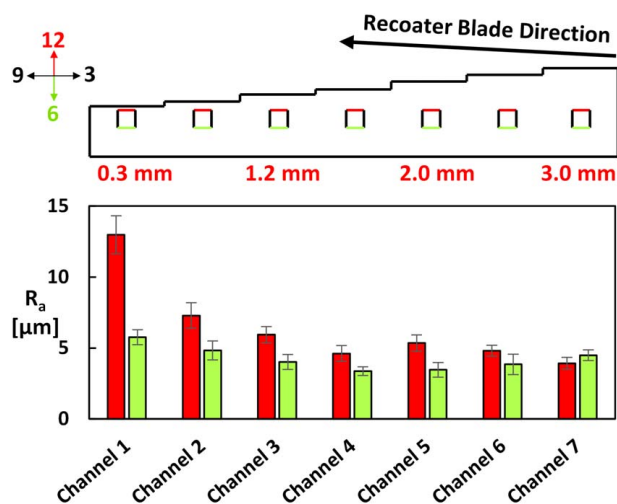


Fig. 2 Arithmetic mean roughness of vertically built square cooling channels at a range of wall thicknesses adapted from Wildgoose et al. [2]

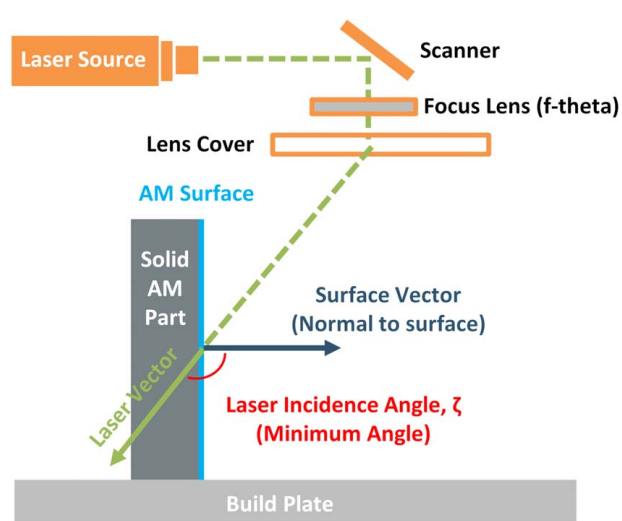


Fig. 3 Definition of laser incidence angle (ζ) using vectors from the lens cover to AM part surface

while the terminal point of the laser vector is the mid-span height of the AM part surface at the build plane. Choosing the center of the lens cover (which is typically directed at the center of the build plate) allows the laser incidence angle to be calculated regardless of the type of focus lens used in the AM machine. The surface vector starting point is at the mid-span height of the AM part surface, while the terminal point is normal to the AM part surface facing away from the solid AM part (into the unsintered powder).

Using the definition in Fig. 3, a standard triangle language (STL) was generated from the design intent computer-aided design (CAD) file for each desired surface inside a single cooling channel. Using an in-house code, a normal vector (facing away from the solid AM part) is placed at the centroid of each STL surface. The laser vector in Fig. 3 is calculated from the origin of the lens cover for each machine to the centroid of each STL surface in the cooling channel. The minimal angle (less than or equal to 180 deg) between the laser vector and surface vector is calculated as the laser incidence angle as shown in Fig. 3. As an example, a cooling channel with a square cross-sectional shape will contain four laser incidence angles due to there being four individual surfaces for the square channel shape.

Wall thickness was also calculated for several samples in the literature. In more detail, the wall thickness is the distance the internal surface of the channel is from the external surface. This definition is similar to what is shown in Figs. 1 and 2. The wall thicknesses reported in this technical brief are AM surfaces that are only parallel to the external surface such as the 12 and 6 o'clock surfaces in Fig. 1(a).

To assess the surface quality of the cooling channels, the internal surface roughness, specifically the arithmetic mean roughness (R_a), was measured using a nondestructive evaluation method known as CT scanning. The arithmetic mean roughness describes the average deviation of a surface from a reference. A commercial CT processing software was used to reduce surface determinations up to one-tenth of the original 35- μm voxel size for the coupons.

3 Impact of Wall Thickness and Laser Incidence Angle on Roughness

The laser incidence angle was analyzed for several cooling passage samples in the literature. The samples chosen for this analysis included noncircular channel shapes such as square cross-sections that were built with no downward-facing surfaces (channel axes are perpendicular to the build plate). More precisely, the samples analyzed include a variety of channel shape cross-sections from Wildgoose et al. [1] as well as square-shaped channel cooling coupons from Wildgoose et al. [8] and Wildgoose et al. [2]. The samples from the studies were fabricated using Inconel 718 with a 40- μm layer thickness. The specific processing parameters used can be found in their respective studies. In addition to the laser incidence angle, the wall thickness was recorded for each sample.

Surface roughness changes according to laser incidence angle as well as wall thickness as seen in Fig. 4. The further the laser incidence angle is from 90 deg the higher the arithmetic mean roughness level. The parabolic trend of roughness as a function of laser incidence angle in Fig. 4 matches the same trend for the flat surface benchmark samples shown by Subramanian et al. [5]. When changing the laser incidence angle from 90 deg to 76 deg, there is a 278% increase in surface roughness at a constant wall thickness of 2 mm, while for the same wall thickness, changing the laser incidence angle from 90 deg to 100 deg causes a 299% increase in surface roughness.

The roughness data points in Fig. 4 are color-coded to their respective wall thicknesses. As such, Fig. 4 allows for a comparison between laser incidence angle and wall thickness on the internal surface roughness of cooling passages. For any given laser incidence angle, the surface roughness increases at wall thicknesses below 1 mm. For samples with wall thickness above 1 mm, the

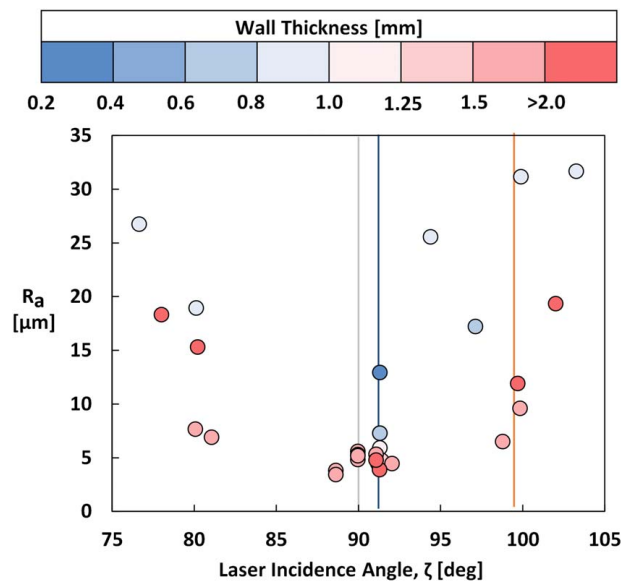


Fig. 4 Arithmetic mean roughness of cooling channel surfaces across a range of wall thickness at two different laser incidence angles from Fig. 3

range in roughness is constant for most samples, which is similar to the results from Wildgoose et al. [2] (Fig. 2).

To evaluate the effect of wall thickness for a given laser incidence angle, Fig. 5 exhibits the impact of wall thickness at a given laser incidence angle. Two laser incidence angles with multiple wall thicknesses from Fig. 4 are shown in Fig. 5. Decreasing the wall thickness causes surface roughness to increase as can be seen when comparing both laser incidence angles in Fig. 5. The surface roughness increased 118% from a 1.2 mm to 0.3 mm wall thickness at a shared laser incidence angle of 91 deg, while the surface roughness increased 350% from 2 mm to a 1.05 mm wall thickness at a shared laser incidence angle of 99 deg. The surfaces in Fig. 5 at a laser incidence angle of 91 deg come from the variable wall thickness sample (shown in Fig. 2) from Wildgoose et al. [2].

Regardless of wall thickness, roughness is higher for surfaces with laser incidence angles furthest from 90 deg. When comparing the same wall thickness but different laser incidence angles in Fig. 5, surface roughness for the 2 mm wall thickness is 30% higher when going from a laser incidence angle of 91–99 deg,

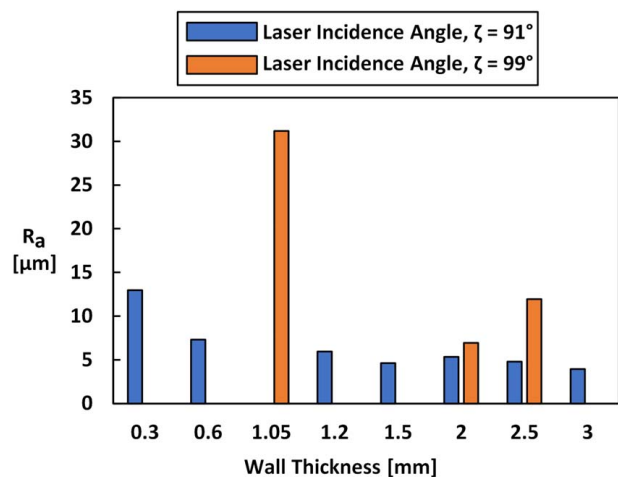


Fig. 5 Arithmetic mean roughness of cooling channel surfaces across a range of wall thickness at two different laser incidence angles from Fig. 4

while the difference in roughness is 85% different when comparing the 2.5 mm wall thickness samples at laser incidence angles between 91 deg and 99 deg. For the two laser incidence angles evaluated in Fig. 5, wall thickness begins to impact surface roughness when wall thickness is below 1 mm.

4 Impact of Wall Thickness and Laser Incidence Angle on Cooling Performance

The cooling performance, specifically the pressure loss (friction factor) and convective heat transfer (Nusselt number) of several samples from the literature [1,8] as shown in Fig. 4, was analyzed to reveal the effect of laser incidence angle and wall thickness on cooling performance. The cooling performance of the samples evaluated was analyzed using the same experimental rig, which has been discussed in detail by Stimpson et al. [10]. The friction factor and Nusselt number were compared for three vertically built coupons fabricated at three different laser incidence angles and at two different wall thicknesses. The design intent hydraulic diameter of 1.25 mm is shared between the square cross-section samples. The coupons evaluated were fabricated on the same EOS machine as well as in Inconel 718 at a 40- μm layer thickness.

The orientation and build location of the samples with respect to the lens cover are shown in Fig. 6(a). There are multiple laser incidence angles in each of the square channel samples in Fig. 6 due to their being four surfaces in a channel (thus four laser incidence angles). Consequently, a range in laser incidence angle is reported for every sample in Fig. 6. In Figs. 6(b) and 6(c), the range in laser incidence angles (ζ) of the samples are 80–100 deg for the S1 sample, 78–102 deg for the S2 sample, and 77–103 deg for the S3 sample. The S1 and S2 samples from Fig. 6 are named R1-3 and R2-1 in the study from Wildgoose et al. [8], while the S3 sample in Fig. 6 is named the square channel shape from Wildgoose et al. [1]. Samples with the highest difference in laser incidence angle from 90 deg were fabricated furthest from the laser source, as shown in Fig. 6(a). The S3 sample is the sample with the greatest range in laser incidence angle from 90 deg and also contains the highest value in arithmetic mean roughness in Fig. 4.

The experimental rig used to measure friction factor and Nusselt number for the samples in Fig. 6 is documented in their respective studies. A comparison of friction factor and Nusselt number between the three samples at a shared fully turbulent Reynolds number of 20,000 is shown in Figs. 6(b) and 6(c). Friction factor and Nusselt number are augmented by the friction factor and Nusselt number of a hydraulically smooth channel. The hydraulically smooth friction factor is calculated from the Colebrook equation [11] with relative roughness equaling zero, while the hydraulically smooth Nusselt number is calculated using the Gnielinski equation [12] with a hydraulically smooth friction factor value.

As seen in Fig. 6(b), a combination of wall thickness and laser incidence angle can impact the friction factor augmentation. As previously reported by Wildgoose et al. [8], friction factor augmentation increases with radial build location which is caused by a greater range in laser incidence angle leading to a greater surface roughness as shown in Fig. 4. Both laser incidence angle range and distance the part is from the laser source (r , radial build location) for the samples as reported in Fig. 6. There is a 6% increase in friction factor augmentation between the S1 and S2 samples; which shared a constant wall thickness of 2.5 mm. The S3 sample contains the thinnest wall thickness (at 1.05 mm) and greatest range in laser incidence angle with respect to the S1 and S2 samples. A combination of the thinnest wall thickness and greatest range in laser incidence angle for the S3 sample causes the friction factor augmentation to be 17% higher compared to the S1 sample.

For the samples in Fig. 5(b), Nusselt augmentation is less dependent relative to friction factor on changes to laser incidence angle or wall thickness. For the S3 sample, which contained the thinnest wall thickness and highest range in laser incidence angle,

the Nusselt augmentation was among the lowest relative to the other samples. The result of Nusselt augmentation not changing with radial build location is in contrast to what has been observed in Wildgoose et al. [8]. Wildgoose et al. [8] showed that there can be a 10% difference between samples fabricated between two different radial build locations. The causes for the lower heat transfer augmentation value of the S3 sample compared to S1 and S2 are related to the type of roughness of the surface. Upon further investigation, the average surface roughness for the S3 sample is 88% higher compared to the S1 and is 44% higher compared to the S2 sample. As reported by Stimpson et al. [13], certain surface roughness features can contribute more to pressure loss and less to convective heat transfer as a result of how well the roughness feature is sintered to the part surface. Characterizing the type of roughness

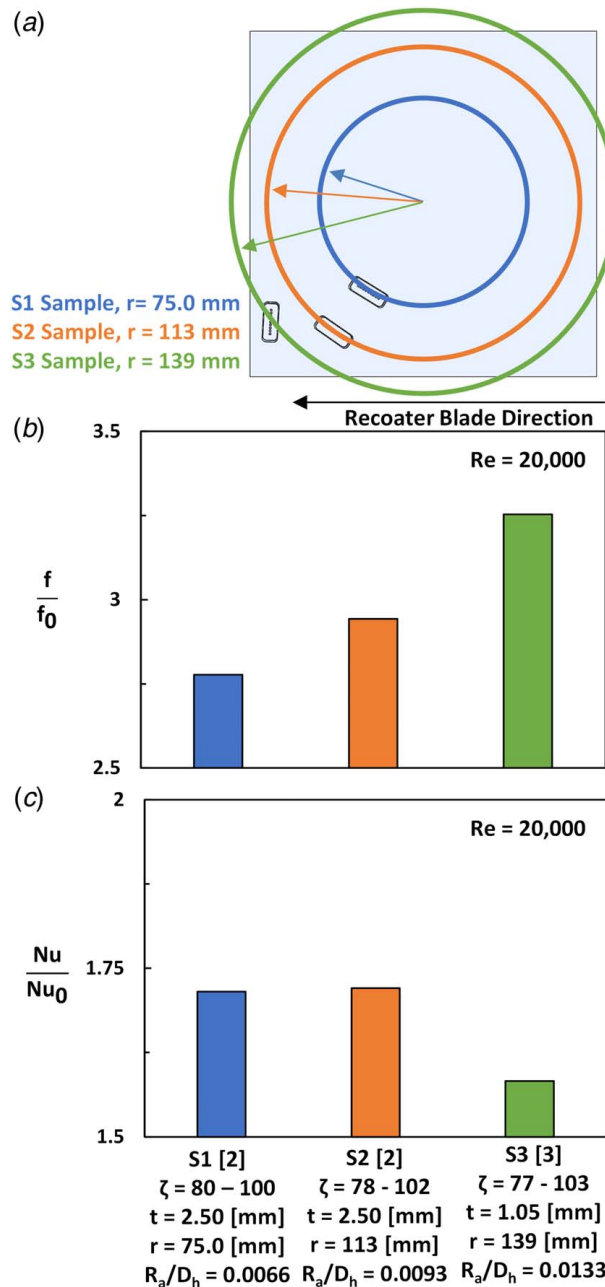


Fig. 6 Schematic of build samples (a) along with friction factor (b) and Nusselt number (c) augmentation of samples [1,7] containing a range of different laser incidence angles and wall thicknesses

and magnitude is important to better understand trends in cooling performance and is an active area of research.

5 Conclusion

Both wall thickness and laser incidence angle affect roughness levels in additively manufactured components. The results from this technical brief show that wall thickness and laser incidence angle are interlinked to the as-built surface roughness of AM cooling channels.

The laser incidence angle was calculated for cooling channel samples with various wall thicknesses previously reported in literature. The arithmetic mean roughness increases as the laser incidence angle becomes further away from 90 deg in a parabolic form. Additionally, for any given laser incidence angle, surface roughness begins to increase when the wall thickness is less than 1 mm for the cooling channels evaluated.

Similar to surface roughness, friction factor changes for different wall thicknesses and laser incidence angles. A range of laser incidence angles can occur for a given cooling passage. Increasing the range of laser incidence angles in a cooling passage causes an increase in the friction factor. Friction factor was found to be highest by lowering the wall thickness from 2.5 to 1 mm and having the greatest range in laser incidence angle. The heat transfer performance, Nusselt number, of the samples evaluated varied less compared to their respective friction factors at a given Reynolds number.

Acknowledgment

The authors would like to acknowledge Penn State's Center for Quantitative Imaging for performing the computed tomography scans.

Conflict of Interest

There are no conflicts of interest.

Data Availability Statement

The authors attest that all data for this study are included in the paper.

Nomenclature

f = Darcy friction factor, $f = \Delta P \frac{D_h}{L} \frac{2}{\rho u_{mean}^2}$
 h = convective heat transfer coefficient, $h = \frac{Q_{in,heater} - \sum Q_{loss}}{A \cdot \Delta T_{lm}}$
 k = thermal conductivity
 r = radial build location
 t = wall thickness
 A = surface area
 L = channel length

T = temperature
 z_{ref} = reference surface plane
 z_{surf} = roughness height
 A_c = cross-sectional flow area
 D_h = hydraulic diameter, $4A_c/p$
 R_a = arithmetic mean roughness, $R_a = \frac{1}{n} \sum_{i=1}^n |z_{surf} - z_{ref}|$
 T_{LM} = log-mean temperature, $\Delta T_{LM} = \frac{(\Delta T_{in} - \Delta T_{out})}{\ln \left(\frac{T_s - T_{in}}{T_s - T_{out}} \right)}$
 Nu = Nusselt number, hD_h/k_{air}

Greek Symbols

ρ = fluid density
 ζ = laser incidence angle

Subscripts

in = inlet condition
 out = exit condition
 s = surface condition

References

- [1] Wildgoose, A. J., and Thole, K. A., 2023, "Heat Transfer and Pressure Loss of Additively Manufactured Internal Cooling Channels With Various Shapes," *ASME J. Turbomach.*, **145**(7), p. 071011.
- [2] Wildgoose, A. J., Thole, K. A., Subramanian, R., Kerating, L., and Kulkarni, A., 2023, "Impacts of the Additive Manufacturing Process on the Roughness of Engine Scale Vanes and Cooling Channels," *ASME J. Turbomach.*, **145**(4), p. 041013.
- [3] Jamshidinia, M., and Kovacevic, R., 2015, "The Influence of Heat Accumulation on the Surface Roughness in Powder-Bed Additive Manufacturing," *Surf. Topogr. Metrol. Prop.*, **3**(1), p. 014003.
- [4] Kleszczynski, S., Ladewig, A., Friedberger, K., Jacobsmuhlen, J. z., Merhof, D., and W. G., 2015, "Position Dependency of Surface Roughness in Parts From Laser Beam," *SFF Symposium Proceedings*, Austin, TX, pp. 360–370.
- [5] Subramanian, R., Rule, D., and Nazik, O., 2021, "Dependence of LPBF Surface Roughness on Laser Incidence Angle and Component Build Orientation," *Proceedings of the ASME Turbo Expo*, American Society of Mechanical Engineers Digital Collection.
- [6] Rott, S., Ladewig, A., Friedberger, K., Casper, J., Full, M., and Schleifenbaum, J. H., 2020, "Surface Roughness in Laser Powder Bed Fusion—Interdependency of Surface Orientation and Laser Incidence," *Addit. Manuf.*, **36**(1), p. 101437.
- [7] Fox, J. C., Moylan, S. P., and Lane, B. M., 2016, "Effect of Process Parameters on the Surface Roughness of Overhanging Structures in Laser Powder Bed Fusion Additive Manufacturing," *Procedia CIRP*, Charlotte, NC, June 8–10, pp. 131–134.
- [8] Wildgoose, A. J., and Thole, K. A., 2022, "Variability in Additively Manufactured Turbine Cooling Features," *J. Glob. Power Propuls. Soc.*
- [9] Alfieri, V., Argenio, P., Caiazzo, F., and Sergi, V., 2017, "Reduction of Surface Roughness by Means of Laser Processing Over Additive Manufacturing Metal Parts," *Materials*, **10**(1), p. 30.
- [10] Stimpson, C. K., Snyder, J. C., Thole, K. A., and Mongillo, D., 2016, "Roughness Effects on Flow and Heat Transfer for Additively Manufactured Channels," *ASME J. Turbomach.*, **138**(5), p. 051008.
- [11] Zigrang, D. J., and Sylvester, N. D., 1985, "A Review of Explicit Friction Factor Equations," *ASME J. Energy Resour. Technol.*, **107**(2), pp. 280–283.
- [12] Gnielinski, 1976, "New Equations for Heat and Mass Transfer in Turbulent Pipe and Channel Flow," *Int. Chem. Eng.*, **16**(2), pp. 359–368.
- [13] Stimpson, C. K., Snyder, J. C., Thole, K. A., and Mongillo, D., 2017, "Scaling Roughness Effects on Pressure Loss and Heat Transfer of Additively Manufactured Channels," *ASME J. Turbomach.*, **139**(2), p. 021003.